J. Chem. Eng. Data 1983, 28, 19–23

Crystal Growth Velocity of Sodium Salt Hydrates

Dan D. Edie,* Charles G. Sandell, and Joseph C. Mullins

Department of Chemical Engineering, Clemson University, Clemson, South Carolina 29631

Salt hydrates are attractive energy storage materials because of their cost and thermophysical properties. Crystal growth data are required to model properly a salt hydrate energy storage system. Growth data for sodium sulfate decahydrate, disodium phosphate dodecahydrate, disodium phosphate heptahydrate, sodium thiosulfate pentahydrate, and sodium carbonate decahydrate are presented.

Introduction

Four sodium salt hydrates (sodium sulfate decahydrate, disodium phosphate dodecahydrate, sodium thiosulfate pentahydrate, and sodium carbonate decahydrate) have a relatively high heat of fusion and have been suggested by Telkes (*1*) as likely candidates for the storage of energy. The thermophysical properties, costs, means of preparation, and nontoxic nature of these materials are all favorable. Trays of these salt hydrates in direct contact with air have been proposed for the storage of energy from solar energy collectors. Direct-contact, immiscible-fluid, batch crystallizers also have been proposed (*2*) as effective heat of fusion energy storage devices. In order to design these energy storage systems, one needs data on the crystal growth rates of these sodium salt hydrates.

Mechanisms of Crystal Growth. The formation of the solid phase from a solution occurs by two mechanisms: nucleation and growth. In the first mechanism crystal embryos lose or add molecules until a specific critical size is reached. Further increase in the size of the crystal begins the second mechanism of crystal growth. The growth of each crystal face proceeds either in a neat uniform layer-upon-layer fashion or by the haphazard propogation of dislocations, dendrites, and eventually occlusions.

As early as 1905 it was proposed that the diffusion of solute molecules through a thin laminar film of liquid adjacent to the growing crystal face is the rate-controlling step for crystal growth (*3*). A few years later it was suggested that the mass deposition rate is controlled by two steps, a diffusion step followed by a surface reaction of order α

$$dM/dt = (D_{AB}/\delta)(C_b - C_i)a = K_c a(C_i - C^*)^\alpha \qquad (1)$$

Therefore, in order to measure the crystal growth rate independent of diffusion effects one must either measure the composition at the solid–liquid interface or else break down the liquid boundary around the growing crystal so that the interfacial liquid composition is nearly equal to the bulk liquid composition.

Coulson and Richardson (*4*) correlated the speed of rotation of a seed crystal suspended in solution to the growth rate of a crystal of sodium thiosulfate. This showed that increased velocities no longer affected the growth rate of the crystal beyond a value of 20 rpm. Yet the crystal growth rate did not become infinite as the thickness of the laminar film was decreased. Instead, it approached a constant value, indicative of the order of the surface reaction rates. Many inorganic salts crystallizing from aqueous solution showed rates slightly greater than first order, while others indicated a second-order reaction rate.

The absorption layer theory of step growth originated by Volmer has been presented by Mullin (*5*). Step growth is the concept of an orderly layer-upon-layer growth with surface nucleation to initiate a new layer. If the crystal surface is molecularly smooth and free from dislocations, then two-dimensional nucleation is required to begin a new layer of molecules. The kinetic law for the growth velocity, V_c, of a perfect crystal face is of the form

$$V_c = A \exp(-B/\Delta T) \qquad (2)$$

The stepwise growth occurs until a critical undercooling is reached, but at larger undercoolings the crystal spontaneously becomes imperfect. As an example, when a perfect stepwise crystal of ice exceeds the 0.65 K undercooling, its growth rate in the direction normal to the basal plane no longer fits the form of eq 2 but becomes

$$V_c = 0.06\Delta T^{1.23} \qquad (3)$$

This result is given by Cahn et al. (*7*).

Hillig and Turnbull (*8*) analyzed the experimental results obtained by several investigators. The growth velocities for several pure liquids at low undercoolings were found to be proportional to the $\Delta T^{1.7}$. The crystal growth velocities measured were the maximum velocities of growth obtained in capillary tubes, observed in the direction parallel to the basal plane.

An imperfection in the growing crystal face can lead to a screw dislocation which eventually becomes a growth spiral. If the crystal grows by this continuous growth mechanism of the screw dislocation, then the growth velocity should be nearly proportional to ΔT^2 (*6*).

Crystal Growth Apparatus. Several authors have described the types of apparatus that can be used to create the laboratory-controlled conditions needed for controlled crystal growth measurement. Bennema (*9*) constructed a crystal growth apparatus designed to record the buoyant mass of a suspended crystal. The boundary layer was minimized on this apparatus by confining all experiments to small undercoolings and thus small growth rates. Mullin (*10*) used a growth cell in which fluid was pumped past a stationary crystal to reduce the diffusion boundary layer. He later used a fluidized-bed crystallizer (*11*) where the relative velocity between the fluid and the crystal was less controlled. McCabe and Stevens (*12*) used a batch crystallizer surrounded by a constant-temperature bath. Since they had many crystals growing within the 1200-mL stirred beaker, the solution concentration changed during the test and fluid velocities were not uniform. In the same study average crystal growth data also were obtained by suspending a cage of seed crystals in a flowing stream of solution and measuring the increase in the crystal mass with time. They noted that the rate of growth of a crystal increased as the relative velocity between the crystal and surrounding solution increased. The increase in growth rate was appreciable at low relative velocities, but, as the relative velocity increased, the increase in growth rate became negligible. The crystal's size only influenced the growth rate when it affected the movement of the crystal within the fluid's velocity profile.

Experimental Section

Since the driving force for crystallization is the degree of supersaturation at the interface, mass and heat transfer resistances which occur during growth tend to decrease this degree of supersaturation. The apparatus used in this study was designed to minimize these effects and at the same time be simple to operate and provide reproducible results. A sche-

0021-9568/83/1728-0019$01.50/0

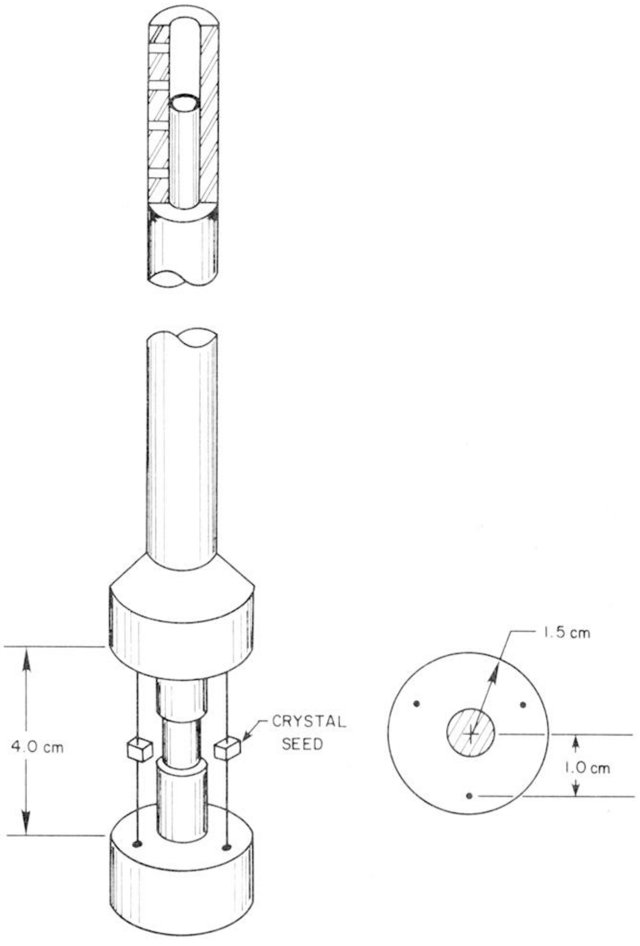

Figure 1. Rotating seed crystal holder.

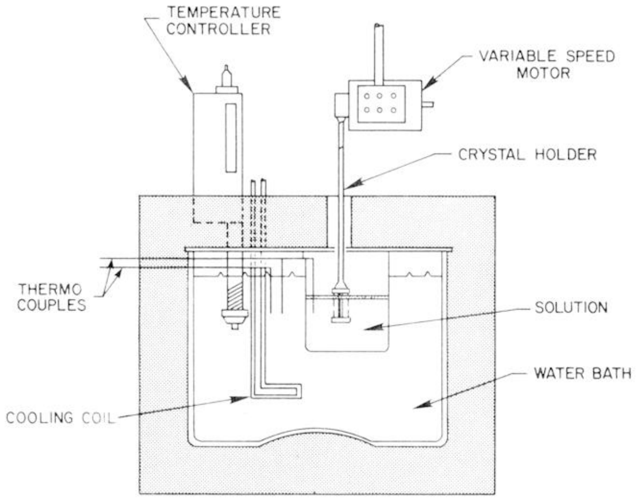

Figure 2. Constant-temperature crystallizer.

Table I. Equilibrium Temperatures

salt	T_{EQ}, K calcd	T_{EQ}, K lit. (ref)
sodium sulfate decahydrate ($Na_2SO_4 \cdot 10H_2O$)	303.98	303.69 (*16*)
disodium phosphate heptahydrate ($Na_2HPO_4 \cdot 7H_2O$)		317.25 (*15*) 318.95 (*17*)
disodium phosphate dodecahydrate ($Na_2HPO_4 \cdot 12H_2O$)	297.54	298.15 (*15*)
sodium carbonate decahydrate ($Na_2CO_3 \cdot 10H_2O$)	302.33	302.04 (*5*)
sodium thiosulfate pentahydrate ($Na_2S_2O_3 \cdot 5H_2O$)	317.74	318.21 (*17*)

matic diagram of the apparatus is shown in Figures 1 and 2. Small crystals were attached to the apparatus using two opposing needle points as shown in Figure 1 and rotated in a supersaturated solution on an axis other than those of the crystals.

The constant-temperature bath consisted of a 20-cm diameter Pyrex glass container covered with a Plexiglas top and surrounded with Styrofoam insulation as shown in Figure 2. The temperature of the water bath was controlled to within ±0.01 K of the desired temperature by using a Haake mercury contact temperature controller. A cooling coil of 9.5-mm o.d. stainless-steel tubing provided a constant refrigeration rate for temperatures below room temperature with control maintained by the heating element of the Haake temperature controller. Temperatures were measured with calibrated thermocouples and a Leeds and Northrop K-3 potentiometer. The rotation of three individual seed crystals within the supersaturated solution was achieved by a variable-speed (up to 550 rpm) electric motor with the seed crystal attached as shown in Figure 2. The center of each seed crystal was 1 cm from the axis of rotation of the crystal holder. A small thermocouple of 30 AWG wire coated with clear varnish was placed in the solution near the revolving crystals. The varnished surface eliminated spontaneous nucleation on the crystalline surface of the wire.

Solutions of Na_2SO_4, Na_2CO_3, and $Na_2S_2O_3$ in deionized water were prepared to concentrations of 30.0, 26.9, and 55.0 mass % of the respective anhydrous salts. For growth experiments on $Na_2HPO_4 \cdot 12H_2O$ and $Na_2HPO_4 \cdot 7H_2O$ solutions of the anhydrous salt in deionized water were prepared to 10.7 and 39.6 mass % of the anhydrous salt. All anhydrous salts were certified ACS grade as supplied by Fisher Scientific Co. The equilibrium temperatures corresponding to these concentrations are listed in Table I. A layer of Dow Corning silicone heat transfer fluid was added to the solution to reduce evaporation.

The salt solution was submerged in the constant-temperature bath, and the temperatures were allowed to equalize over a period of 6–8 h. The constant-temperature-bath temperature returned to the steady-state temperature slightly below the anticipated equilibrium temperature. The masses of three small seed crystals (8.0 mm^3 or less), grown in a saturated solution, were carefully determined. These crystals were washed in a *sec*-butyl alcohol solution and dried prior to weighing. The crystals were mounted on the apparatus between the needle points. Prior to the immersion of the seed crystals in the undercooled solution, the crystals were suspended in the vapor space above the solution for 40 min to allow the Plexiglas holder and crystals to attain the same temperature as the solution. Once the crystals were immersed, the rotation of the seed crystals began the timed growth period. The rotation speed was increased during the first 30 s and decreased during the last 30 s of the 10-min growth period. The initial and final mass of the crystal was measured with a precision of ±0.001 mg. A detailed description of the experimental procedure is given by Sandell (*13*). The possibility of occluded water and/or the presence of different hydrate crystal forms within the same hydrate crystal was determined by using the analytical procedure given by Kolthoff and Sandell (*14*).

Results

The results of this investigation give the average linear growth rates as a function of undercooling for the four sodium salt compounds tested. Preliminary information was obtained for the growth rate of sodium sulfate decahydrate as a function of the rotation speed. The results are shown in Figure 3. Above 240 rpm the growth rate of sodium sulfate decahydrate is nearly independent of rotation speed. Therefore, subsequent measurements on sodium sulfate decahydrate were made at 240 rpm. Similar tests were performed with the other sodium salt

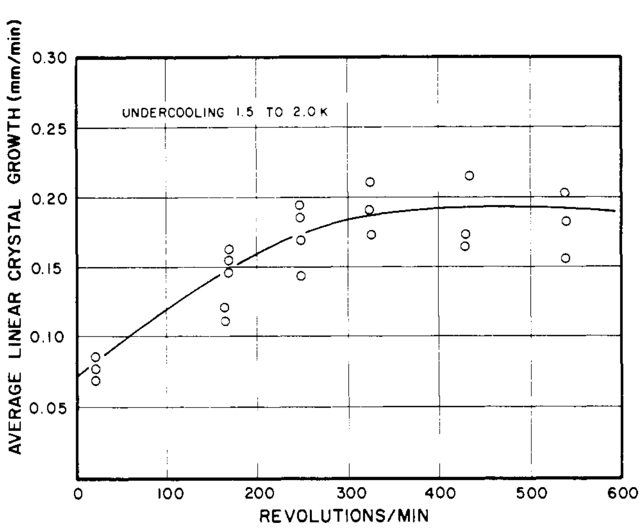

Figure 3. Average linear crystal growth rate of sodium sulfate decahydrate in a 30.0 mass % solution as a function of revolutions per minute.

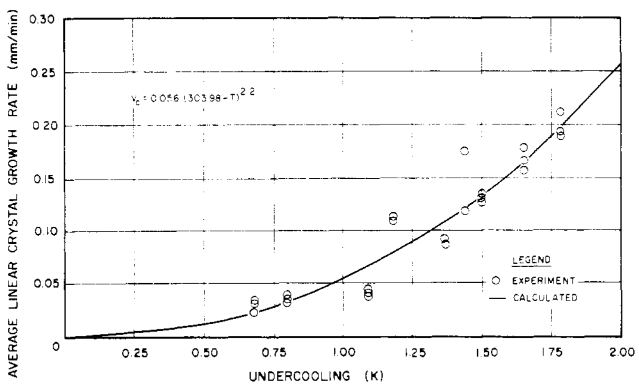

Figure 4. Average linear crystal growth rate of sodium sulfate decahydrate in a 30.0 mass % solution as a function of undercooling.

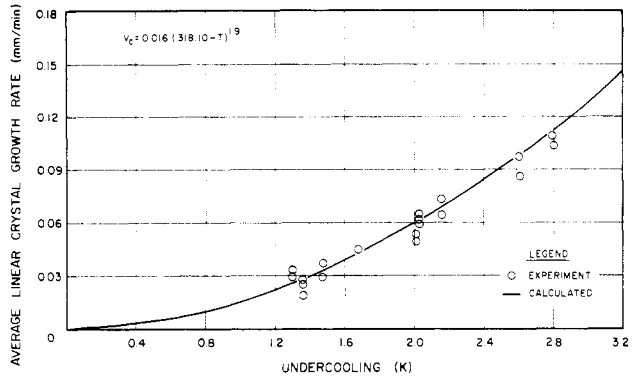

Figure 5. Average linear crystal growth rate of disodium phosphate heptahydrate in a 39.6 mass % solution as a function of undercooling.

hydrates. For each system these provided the rotation speed necessary to ensure that crystal growth rate was independent of rotation speed.

Crystal Growth Velocity vs. Undercooling. Below 1.50 K undercooling the nucleation rate for sodium sulfate decahydrate was negligible compared to the crystal growth rate. The data obtained in this region are shown in Figure 4. The measured crystal growth rates are at rotation speeds of 240 rpm; consequently, they represent the crystal surface reaction rate plus the limitations of a thin boundary layer.

The disodium phosphate solution forms two separate crystal phases, the dodecahydrate and the heptahydrate. Therefore, the phase diagram was consulted for the specific concentration and temperature range needed to limit the solidification to one form or another (*15*). Consequently, two sets of data and two separate plots, Figures 5 and 6, are shown for the crystal system.

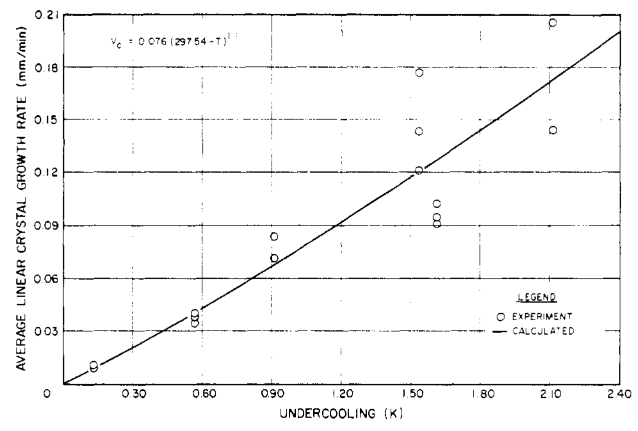

Figure 6. Average linear crystal growth rate of disodium phosphate dodecahydrate in a 10.7 mass % solution as a function of undercooling.

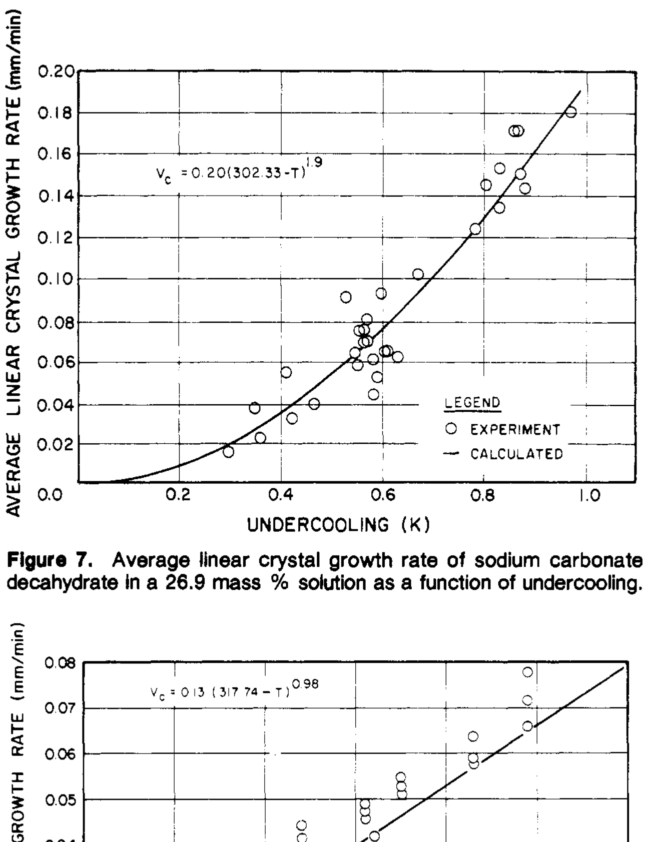

Figure 7. Average linear crystal growth rate of sodium carbonate decahydrate in a 26.9 mass % solution as a function of undercooling.

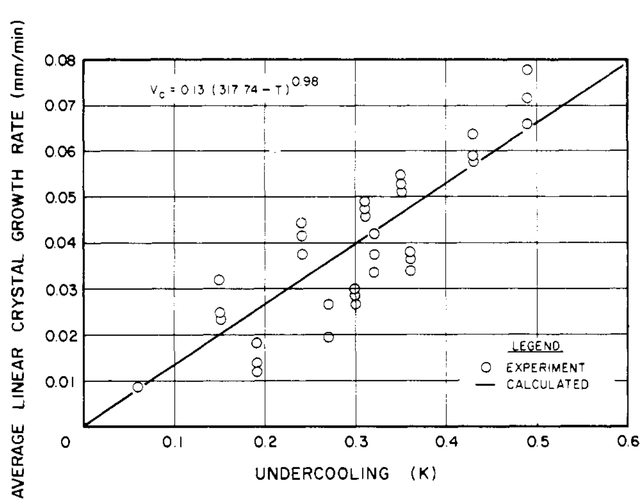

Figure 8. Average linear crystal growth rate of sodium thiosulfate pentahydrate in a 55.0 mass % solution as a function of undercooling.

The sodium carbonate decahydrate crystal grows faster than the sodium sulfate decahydrate. Therefore, it required faster rotation speeds to eliminate the boundary layer resistances. Above 0.5 K undercooling, the rpm was increased to 320. Beyond 1.0 K undercooling the solution had a tendency to nucleate spontaneously. Data for this system are shown in Figure 7.

Growth rate data from the sodium thiosulfate pentahydrate system are plotted in Figure 8. This system is not easy to nucleate spontaneously and, because of this, gave excellent well-formed seed crystal growth.

Discussion

The assumptions made during the conversion of mass growth data to linear velocity, the effect of mass transfer on the results, and the form of a crystal growth velocity equation are factors which affect the interpretation of the data.

Characteristic Shape Factor. Each seed crystal selected to initiate the growth surfaces had its own particular shape. They ranged in mass from 0.0137 to 0.537 g. When viewed under a microscope with a magnification of 100×, the surface of even the smoothest seed crystal appeared to have a number of irregularities. Consequently, a visual observation of a salt hydrate crystal failed to yield an absolutely characteristic dimension that could be directly measured. Instead, the mass of a given crystal was determined and the density of a given crystal hydrate form was used to calculate the characteristic volume that it occupied. Using the shape of a cube, we determined the characteristic side dimensions to give the overall average linear crystal growth rate. A characteristic cube was chosen because it closely resembles the shape of the seed crystals.

The actual surface area exposed is larger for the irregular shape than it is for the characteristic cube. The opportunity for the growth of the crystal is directly related to the amount of surface area exposed. So, for a comparison of the growth velocities of two crystals of identical mass, they must both possess the same degree of irregularity. This uncontrolled feature of the characteristic dimension caused some scatter around a statistical mean value. Because of this difference, the three seed crystals exposed to the exact same crystal growth conditions did not grow at the same rate. Nevertheless, the data obtained in all but a few cases reveal that the three crystals exposed to the same growth environment exhibited growth velocities which differed by less than ±0.020 mm/min at undercoolings less than 1.0 K.

Limiting Rotation Speeds. Before the surface reaction rate for the crystallization process is measured, it is necessary to show that the growth conditions are not controlled by the diffusion of solute across a laminar boundry layer. Mullin and Gaska (*11*), in their study of the effect of solution velocity on the growth rate of potassium sulfate crystals, found that above a relative velocity of about 16 cm/s the growth rate became more or less independent of the relative velocity.

A rotation speed of 240 rpm, corresponding to a crystal velocity of 25 cm/s, was found to be satisfactory for measuring the growth velocity of crystals of sodium sulfate decahydrate at undercoolings of less than 1.5 K. The other crystals (disodium phosphate decahydrate and heptahydrate, sodium carbonate decahydrate, and sodium thiosulfate pentahydrate) were grown first at 240 rpm and then at faster rotation speeds. Because of the higher growth velocity of sodium carbonate, it was necessary to increase the speed of rotation to 320 rpm to eliminate the effect of rotation on the results. There appears to be no easy way to be certain that mass transfer through the laminar sublayer does not affect the final results to some extent.

Crystal Growth Velocity Equations. Since past studies have shown growth velocity to be proportional to a power of the undercooling (except for extremely low undercoolings), eq 4 was chosen to correlate the data. A fit of the crystal growth rate data gives the exponent term, the constant term, and the equilibrium temperature for the equation

$$V_c = A(T_{EQ} - T)^{\alpha} \qquad (4)$$

Table II. Standard Deviation of Coefficients

salt	A	α	T_{EQ}
sodium sulfate decahydrate ($Na_2SO_4 \cdot 10H_2O$)	0.100	1.40	0.81
disodium phosphate heptahydrate ($Na_2HPO_4 \cdot 7H_2O$)	0.002	0.19	
disodium phosphate dodecahydrate ($Na_2HPO_4 \cdot 12H_2O$)	0.040	0.50	0.42
sodium carbonate decahydrate ($Na_2CO_3 \cdot 10H_2O$)	0.070	0.58	0.20
sodium thiosulfate pentahydrate ($Na_2S_2O_3 \cdot 5H_2O$)	0.016	0.11	0.33

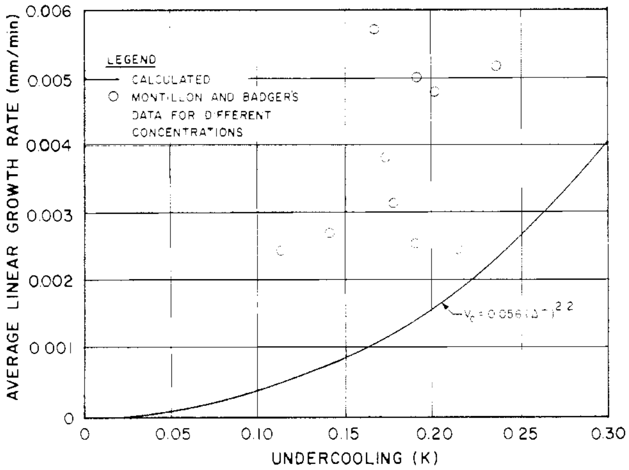

Figure 9. Comparison of the sodium sulfate growth rate equation with the growth rate data obtained by Montillon and Badger (*16*) using a continuous crystallizer apparatus.

The optimum values of A, α, and T_{EQ} were found by a regression analysis of the data and the standard deviations for these constants for each salt system are given in Table II. The final equations are given in the figures for each salt hydrate.

The equilibrium temperatures as estimated by regression analysis of the data for four of the salt hydrates are compared with values found in the literature in Table I. The excellent agreement between these values is a further check on the consistency of the growth data. However, the growth data from one salt hydrate (disodium phosphate heptahydrate) were not precise enough to confidently determine the equilibrium temperature by regression analysis. Therefore, the equilibrium temperature was assumed to be the average of those literature values listed in Table I and then a regression analysis of the data yielded the constants A and α in eq 4.

The literature contains very few data on the growth rate of sodium salt hydrates but comparison of the sodium sulfate decahydrate growth rate equation with the data obtained by Montillon and Badger (*16*), using a continuous crystallizer apparatus, is shown in Figure 9. The data compiled by Montillon and Badger are used by calculating the proportion of mass increase attributable to one average-size seed crystal. The typical crystal's mass before and after the timed growth period gives the linear growth rate for the specified undercooling. The sodium sulfate decahydrate equation predicts a slightly lower growth rate than the results of Montillon and Badger. Since Montillon and Badger's data were taken over a range of undercooling of 0.1–0.24 K and the data in the present study cover undercoolings of 0.2–1.9 K, exact agreement would not be expected. Even the mode of crystal growth can vary as the range of undercoolings varies. Also, the crystallizer used by Montillon and Badger varied by 0.2 °C over its length (nearly as much as the total estimated undercooling).

Mullin (*5*) states that many inorganic salts crystallizing from aqueous solutions show rates slightly greater than first order, while others indicate a second-order reaction. The three salt hydrates (sodium sulfate decahydrate, sodium carbonate decahydrate, and disodium phosphate heptahydrate) are examples of the second-order reaction case while the growth of disodium phosphate dodecahydrate and sodium thiosulfate appears to be first order.

Conclusions

The results of this investigation support the following conclusions for the sodium salt hydrate crystals.

1. When a velocity differential of from 25 to 30 cm/s is maintained between the crystal and the fluid solution, the average linear growth velocity is independent of crystal size.

2. The average linear crystal growth velocities, V_c, for the five disodium salt hydrate crystals are measured in terms of the degrees Celsius undercooling ΔT to be the following:

(a) sodium sulfate decahydrate

$$V_c = 0.056\Delta T^{2.2}$$

$$T_{EQ} - T = \Delta T \leq 1.8 \text{ K}$$

$$T_{EQ} = 303.98 \text{ K}$$

(b) disodium phosphate heptahydrate

$$V_c = 0.016\Delta T^{1.9}$$

$$T_{EQ} - T = \Delta T \leq 2.2 \text{ K}$$

$$T_{EQ} = 318.10 \text{ K}$$

(c) disodium phosphate dodecahydrate

$$V_c = 0.076\Delta T^{1.1}$$

$$T_{EQ} - T = \Delta T \leq 2.1 \text{ K}$$

$$T_{EQ} = 297.54\ k$$

(d) sodium carbonate decahydrate

$$V_c = 0.20\Delta T^{1.9}$$

$$T_{EQ} - T = \Delta T \leq 1.0 \text{ K}$$

$$T_{EQ} = 302.33 \text{ K}$$

(e) sodium thiosulfate pentahydrate

$$V_c = 0.13\Delta T^{0.98}$$

$$T_{EQ} - T = \Delta T \leq 0.73 \text{ K}$$

$$T_{EQ} = 317.74 \text{ K}$$

These measurements are for seed crystals exposed to a fluid velocity sufficient to minimize the boundry layer thickness.

Acknowledgment

We thank D. J. Kirwan for helpful discussions about planning the experiments.

Glossary

M	mass, g
t	time, s
a	surface area of the crystal face, m^2
C	bulk solution concentration, g/m^3
C_i	solid–liquid interface concentration, g/m^3
C^*	equilibrium saturation concentration, g/m^3
D_{AB}	diffusion coefficient, m^2/s
δ	boundary layer thickness, m
α	order of the surface reaction, dimensionless
V_c	crystal growth, mm/min
A	constant, mm/min
B	constant, K
ΔT	undercooling ($T_{EQ} - T$), K
T_{EQ}	equilibrium freezing temperature, K
T	solution temperature, K

Literature Cited

(1) Telkes, M. *ASHRAE J.* **Sept 1974**, *16*, 38–44.
(2) Edie, D. D.; Melsheimer, S. S. "Proceedings of the International Solar Energy Society"; The American Section of the International Solar Energy Society: Cape Canaveral, FL, 1976; Vol. 8, pp 262–72.
(3) Nernst, W. *Z. Phys. Chem.* (*Leipzig*) **1905**, *47*, 52.
(4) Coulson, J. M.; Richardson, R. F. "Chemical Engineering"; McGraw-Hill: New York, 1955; Vol. II, pp 817–8.
(5) Mullin, J. W. "Crystallisation", 2nd ed.; Butterworths: London, 1972; pp 154–8, 249.
(6) Kirwan, D. F. Ph.D. Dissertation, University of Delaware, Newark, DE, 1967.
(7) Cahn, J. W.; Hillig, W. B.; Sears, G. W. *Acta. Metall.* **1964**, *12*, 1421–39.
(8) Hillig, W. B.; Turnbull, D. *J. Chem. Phys.* **1956**, *24*, 914.
(9) Bennema, P. Phys. *Status Solidi* **1966**, *17*, 555–62.
(10) Mullin, J. W.; Garside, J. *Trans. Inst. Chem. Eng.* **1967**, *45*, 285–90.
(11) Mullin, J. W.; Gaska, C. *Can. J. Chem. Eng.* **1969**, *47*, 483–9.
(12) McCabe, W. L.; Stevens, R. P. *Chem. Eng. Prog.* **1951**, *47*, 168–74.
(13) Sandell, C. G. M.S. Thesis, Clemson University, Clemson, SC, 1977.
(14) Kolthoff, I. M.; Sandell, E. B. "Textbook of Quantitative Inorganic Analysis", 3rd ed.; Macmillan: New York, 1952; pp 138–48.
(15) Timmermans, J. "The Physico-Chemical Constants of Binary Systems in Concentrated Solution"; Interscience: New York, 1960; Vol. III, p 405.
(16) Montillon, T.; Badger, W. L. *Ind. Eng. Chem.* **1927**, *19*, 809–16.
(17) Washburn, E. W. "International Critical Tables of Numerical Data, Physics, Chemistry and Technology"; McGraw-Hill: New York, 1926; Vol. IV, pp 236–7.

Received for review March 29, 1982. Accepted September 29, 1982. This work was supported by the U.S. Department of Energy under contract No. EY-76-S-05-5190 to Clemson University.